

Article

Preparation of Metal Coatings on Steel Balls Using Mechanical Coating Technique and Its Process Analysis

Liang Hao ^{1,2}, Hiroyuki Yoshida ³, Takaomi Itoi ⁴ and Yun Lu ^{4,*}

¹ Tianjin Key Lab. of Integrated Design and On-Line Monitoring for Light Industry & Food Machinery and Equipment, Tianjin 300222, China; haoliang@tust.edu.cn

² College of Mechanical Engineering, Tianjin University of Science and Technology, No. 1038, Dagu Nanlu, Hexi-District, Tianjin 300222, China

³ Chiba Industrial Technology Research Institute, 6-13-1, Tendai, Inage-ku, Chiba 263-0016, Japan; h.yshd14@pref.chiba.lg.jp

⁴ College of Mechanical Engineering & Graduate School, Chiba University, 1-33, Yayoi-cho, Inage-ku, Chiba 263-8522, Japan; itoi@chiba-u.jp

* Correspondence: luyun@faculty.chiba-u.jp; Tel.: +81-43-290-3514

Academic Editors: Tony Hughes and Russel Varley

Received: 1 February 2017; Accepted: 7 April 2017; Published: 10 April 2017

Abstract: We successfully applied mechanical coating technique to prepare Ti coatings on the substrates of steel balls and stainless steel balls. The prepared samples were analyzed by X-ray diffraction (XRD) and scanning electron microscopy (SEM). The weight increase of the ball substrates and the average thickness of Ti coatings were also monitored. The results show that continuous Ti coatings were prepared at different revolution speeds after different durations. Higher revolution speed can accelerate the formation of continuous Ti coatings. Substrate hardness also markedly affected the formation of Ti coatings. Specifically, the substance with lower surface hardness was more suitable as the substrate on which to prepare Ti coatings. The substrate material plays a key role in the formation of Ti coatings. Specifically, Ti coatings formed more easily on metal/alloy balls than ceramic balls. The above conclusion can also be applied to other metal or alloy coatings on metal/alloy and ceramic substrates.

Keywords: Ti coatings; steel balls; mechanical coating; process analysis

1. Introduction

Coating technology is one of the most frequently-used surface modification technologies, and has been applied in many engineering fields, including corrosion prevention [1], thermal barrier [2,3], anti-friction [4,5], stealth materials [6], etc. Other functions such as photocatalytic activity have also been found in metal/alloy coatings after certain treatments including thermal oxidation [7,8], chemical oxidation [9,10], plasma electrolytic oxidation [11,12], anodic oxidation [13,14], among others. In our published work, we prepared TiO₂/Ti composite photocatalyst coatings on the substrate of Al₂O₃ balls using mechanical coating followed by thermal oxidation [15]. With further study, we developed oxygen-deficient visible-light-responsive TiO₂ coatings [16]. Therefore, the preparation of metal/alloy coatings is of paramount practical importance. Researchers have prepared several kinds of metal/alloy coatings on ceramic or metal substrates using mechanical coating technique [17]. Early in 1995, Kobayashi developed Al and Ti-Al coatings on the substrates of stainless steel balls and ZrO₂ balls [18]. Romankov et al. [19] also prepared Al and Ti-Al coatings on a Ti alloy substrate. Gupta et al. [20] prepared nanocrystalline Fe-Si alloy coatings on a mild steel substrate. Farahbakhsh et al. [21] deposited Cu and Ni-Cu solid solution coatings on ceramic and metal substrates. We have fabricated Fe and Zn

coatings on Al₂O₃ ball substrates [22,23]. Furthermore, we have also revealed that the properties of the metal powder played an important role in the formation of metal coatings [24]. Besides the influence of some processing parameters including milling speed and time, a possible mechanism of coatings' formation was further studied in [20,21,23].

However, the influence of substrates including material properties and surface roughness on the formation of metal coatings has not been revealed so far. In this work, we would verify the formation possibility of metallic coatings on metallic substrates and attempted to prepare Ti coatings on different steel substrates utilizing mechanical coating technique. The formation process of Ti coatings and the influence of substrates' properties on their formation were also involved.

2. Materials and Methods

Ti coatings were prepared using a mechanical coating technique with a planetary ball mill (Pulverisette 6, Fritsch). The transmission ratio of the mill was 1:–1.82. Ti powder (Osaka Titanium Technologies Co. Ltd., Osaka, Japan) and steel balls as the substrates were charged into a bowl made of alumina (volume: 250 mL). The bowl was fixed in the planetary ball mill, and then the mechanical coating process was carried out at different rotational speeds for different durations. Two kinds of substrates were used separately to clarify the influence of steel ball substrates on the formation of metal coatings, including steel balls (SUJ-2, density of 7.85 g·cm^{–3}) and stainless steel balls (SUS-304, density of 7.93 g·cm^{–3}). The composition of steel (SUJ-2) and stainless steel balls (SUS-304) is listed in Table 1. To study the influence of substrates' surface roughness, steel balls were polished to make their surface smoother before the mechanical coating process. The polishing process is as follows. Firstly, abrasive paper with mesh number of 80 was put into the bowl along the wall of the bowl. Secondly, the balls were charged into the bowl and ball milling was carried out. In the ball milling, the balls were polished by the abrasive paper throughout their repeated collision and friction with the ball of the bowl. The surface roughness of the balls was not measured. Meanwhile, steel balls were annealed in vacuum at 1073 K holding for 1.5 h to change their hardness before mechanical coating process to study the influence of the substrate hardness on the coatings' formation. Tables 2 and 3 give the relevant processing parameters and the sample symbols. The average particle size distribution of titanium powder is about 30 μm, ranging from 5–100 μm. Most of them (up to 70%) are located in the range of 20–50 μm. The parameters *x* and *y* correspond to the rotational speed of the mill and milling time, respectively. The volume ratio of metallic powder to the balls and the filling degree are 1:1.7 and 5%, respectively.

Table 1. Composition of steel (SUJ-2) and stainless steel (SUS-304) balls in the work.

No.	C	Si	Mn	P	S	Ni	Cr	Others
SUJ-2	0.95–1.10	0.15–0.35	≤0.50	≤0.025	≤0.025	–	1.30–1.60	Fe
SUS-304	≤0.08	≤1.00	≤2.00	≤0.045	≤0.030	8.00–10.50	18.00–20.00	Fe

Table 2. Relevant processing parameters in the present work.

Raw Materials		Weight (g)	Average Diameter (mm)	Purity (%)
Metal powder	Ti powder	20.0	0.03	99.1
Substrates	Steel balls	58.5	1.0	SUJ-2
	Stainless steel balls	59.5	1.0	SUS-304

Table 3. Relevant sample symbols and treatment condition of the balls in the present work.

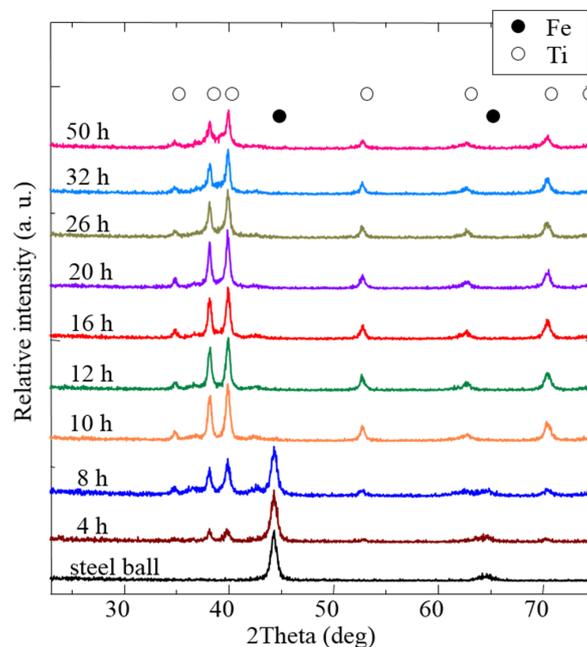
Sample Symbol	Substrate	Surface Roughness	Hardness (HV)
TSx-y	SUJ-2	original	809
TSSx-y	SUJ-2	polished	809
TSYx-y	SUJ-2	original	201
TBx-y	SUS-304	original	187

All samples were characterized by X-ray diffractometer (XRD) (JDX-3530, JEOL, Tokyo, Japan) with Cu K α radiation at 30 kV and 20 mA to determine the phases present. A scanning electron microscope (SEM) (JSM-6510A, JEOL, Tokyo, Japan) was used to observe the surface morphologies and the microstructure of the cross-sections of the Ti-coated steel balls. The average thickness of Ti coatings was estimated from 40 different locations of five Ti-coated steel balls in their SEM images of the cross sections. The average weight increase of 50 steel balls during mechanical coating process was also calculated by weighing 50 randomly-selected Ti-coated steel balls three times.

3. Results and Discussion

3.1. Preparation of Ti Coatings on Steel Balls

The XRD patterns of the Ti-coated steel balls are presented in Figure 1. We could see the diffraction peaks of Ti in addition to those of Fe from the XRD patterns when the duration of mechanical coating processing was increased to 4 and 8 h. This means that some Ti powder particles adhered to the surface of the steel balls. When processing time reached 10 h, the diffraction peaks of Fe could no longer be observed, indicating that continuous Ti coatings had formed on the steel balls.

**Figure 1.** XRD patterns of the Ti coatings prepared by mechanical coating on steel balls at 300 rpm.

The surface morphologies of Ti-coated steel balls were recorded by SEM and are displayed in Figure 2. When the duration of the mechanical coating process was 4 and 8 h, Ti powder particles discontinuously coated the surfaces of steel balls (Figure 2a,b). With the increase of process duration to 10 h, continuous Ti coatings formed (Figure 2c). The surface of the Ti coatings became rugged, and humps were formed with further increase of duration to 50 h. The results from the SEM images

are consistent with that reflected from the XRD patterns in Figure 1. Figure 3 shows the SEM images of the cross-section of the samples prepared by mechanical coating. Although the coating of Ti powder particles on steel balls was not clearly observed (Figure 3a,b) when the duration was 4 or 8 h, the formation of continuous Ti coatings was confirmed after 8 h of mechanical coating (Figure 3c). The coatings' evolution in Figure 3 agreed with that in Figures 1 and 2. Therefore, we can say that continuous Ti coatings on steel balls were prepared at 300 rpm after 10 h of mechanical coating process from the above results.

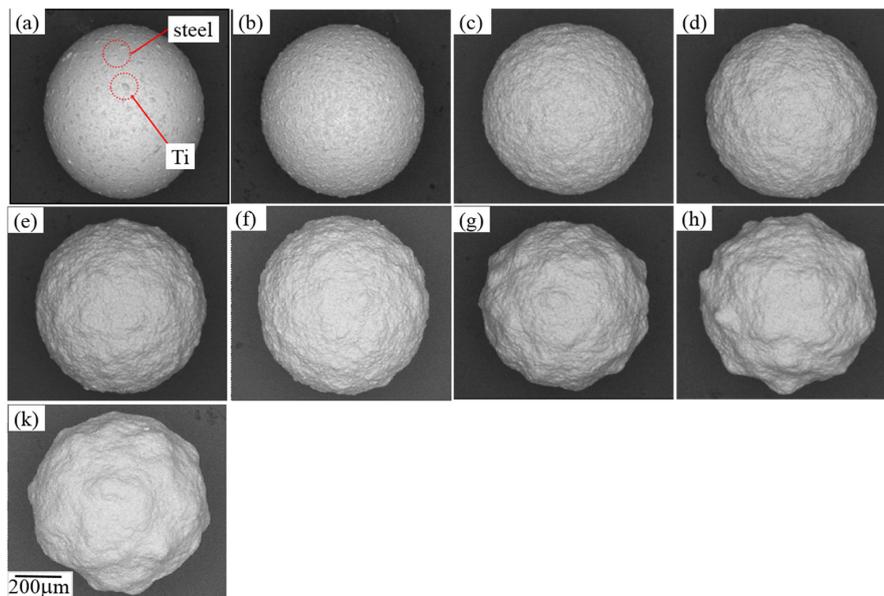


Figure 2. SEM images for the surface morphologies of the samples prepared by mechanical coating at 300 rpm after different duration: (a) 4 h; (b) 8 h; (c) 10 h; (d) 12 h; (e) 16 h; (f) 20 h; (g) 26 h; (h) 32 h; and (k) 50 h.

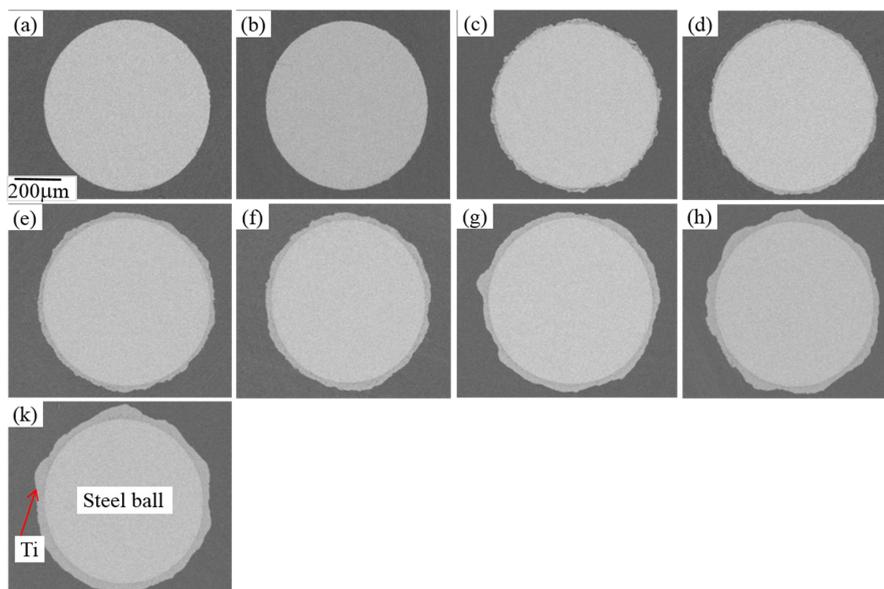


Figure 3. SEM images for the cross-section of the samples prepared by mechanical coating at 300 rpm after different durations: (a) 4 h; (b) 8 h; (c) 10 h, (d) 12 h; (e) 16 h; (f) 20 h; (g) 26 h; (h) 32 h; and (k) 50 h.

3.2. Influence of Rotational Speed

To study the influence of revolution speed on the formation of Ti coatings, continuous Ti coatings on steel balls were also prepared at 400 rpm, with the results displayed in Figure 4. We can see that continuous Ti coatings have been formed after 4 h of the mechanical coating process (Figure 4b). The thickness of the Ti coatings was increased with the increase of duration from 4 h to 20 h. However, continuous Ti coatings began to separate from steel balls as the duration was further increased to 26 and 32 h. Therefore, we can say the evolution includes the following four stages: nucleation, growth of nuclei, formation of coatings, and exfoliation. The evolution is similar to that of Fe and Zn coatings [22,23].

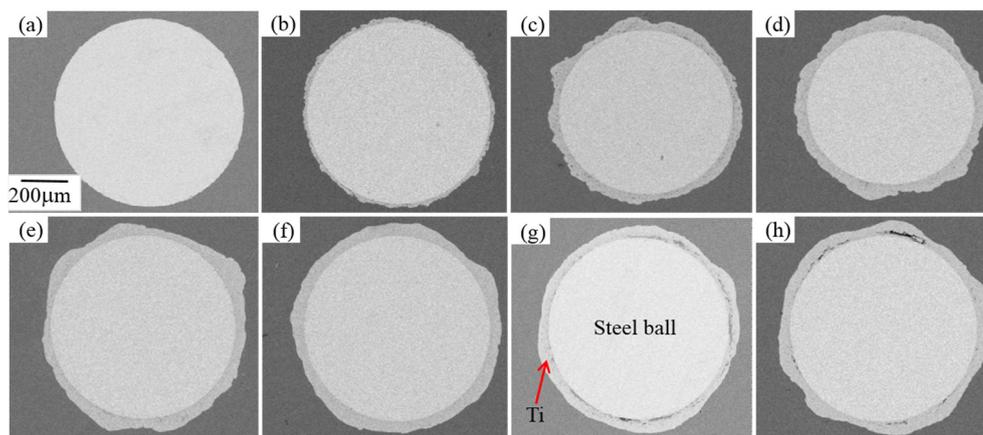


Figure 4. SEM images for cross-section of Ti samples prepared by mechanical coating at 400 rpm after different durations: (a) 1 h; (b) 4 h; (c) 8 h; (d) 12 h; (e) 16 h; (f) 20 h; (g) 26 h; and (h) 32 h.

The weight increase of 50 steel balls during mechanical coating at different revolution speeds was recorded as illustrated in Figure 5. The weight increase means that more Ti powder particles coat the steel balls. We found that the weight of the steel balls increased with the increase in duration. However, the weight increase became greater with the increase of revolution speed from 200 to 400 rpm at the same mechanical coating process duration. This suggests that a higher revolution speed can accelerate the coating of Ti powder particles on the surface of steel balls. The average thickness change of continuous Ti coatings was also monitored as shown in Figure 6. We can note that the data at 200 rpm is absent because continuous Ti coatings were not even successfully prepared after 50 h. This hints that continuous Ti coatings may not be formed at revolution speeds of 200 rpm or lower. The average thickness evolution of continuous Ti coatings at 300 and 400 rpm is similar to the weight increase change in Figure 5. When rotational speed was 400 rpm, the weight began to decrease when the time came to 26 h, as the formed coatings began to peel off. If milling time is prolonged any further, the exfoliation of metallic coatings will continue. Therefore, we did not provide data after 26 h. According to the parameters named “collision strength” and “collision power” which we proposed in published work [23], the energy transferred to the metallic powder particles from the balls quickly increases with the increase of rotation speed of the ball mill. Greater collision power means larger transferred collision energy, which creates severe plastic deformation. The cold welding among metallic powder particles occurs only when plastic deformation is greater than a critical value [24].

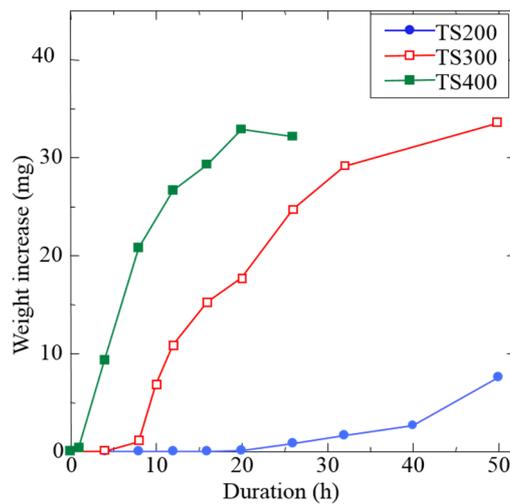


Figure 5. Weight increase of 50 steel balls versus duration of mechanical coating at different revolution speeds.

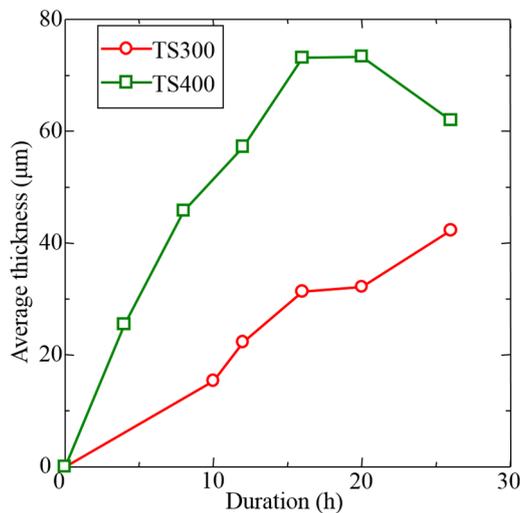


Figure 6. Average thickness of Ti coatings versus duration of mechanical coating at different revolution speeds.

3.3. Influence of Surface Roughness and Hardness

The SEM images for the morphologies of the samples prepared by the mechanical coating process are shown in Figure 7. Figure 7a,b show the influence of surface roughness on the coatings' formation. No evident difference can be observed from the SEM images. From Figure 8, we can see that the initial coating rate for the polished balls was slightly greater than those which were unpolished. In other words, the decrease in surface roughness favors the adhesion of metallic powder particles to the surface of metallic balls. We believe that the surface roughness improvement can decrease the air volume reserved in the cavities in the surface of the balls. The contact area among the balls and the metallic powder particles was increased, which can increase the possibility of cold welding. Therefore, the surface roughness improvement accelerated the formation of metallic coatings. On the other hand, surface roughness improvement decreased the quantity of the cavities in the surface. Therefore, the interaction opportunity—specifically the mechanical inter-locking between the cavities and the metallic particles—was decreased. Finally, the surface roughness improvement hinders the formation of metallic coatings. According to the above results, we can conclude that the influence of the surface roughness on the formation of metallic coatings is rather complex; the coexistence of promoting and

obstructive factors made the influence negligible. As for the influence of the substrates' hardness, the formation situation of Ti coatings is given in Figure 7c,d. We can clearly see that more Ti powder particles were adhered to the annealed steel ball than to the steel ball. In other words, Ti powder particles more easily coat the softer steel balls. A slight difference in weight increase shown in Figure 8 also proved this. The influence of balls' surface hardness on the coating of metallic powder particles can also be attributed to the cold welding of metallic powder. As discussed above, the cold welding among balls and metallic powder particles happens only when a critical plastic strain is satisfied. After they were annealed, the balls became softer than that before annealing. During the collision among balls and metallic powder particles, the softer surface of the balls welds with the metallic particles more easily. After the surface of these balls is totally coated with metallic powders after 12 h of ball milling, the interaction among balls and metallic powder particles has been replaced by that among metallic powder particles. Therefore, the influence of surface parameters including roughness and hardness cannot be studied any more.

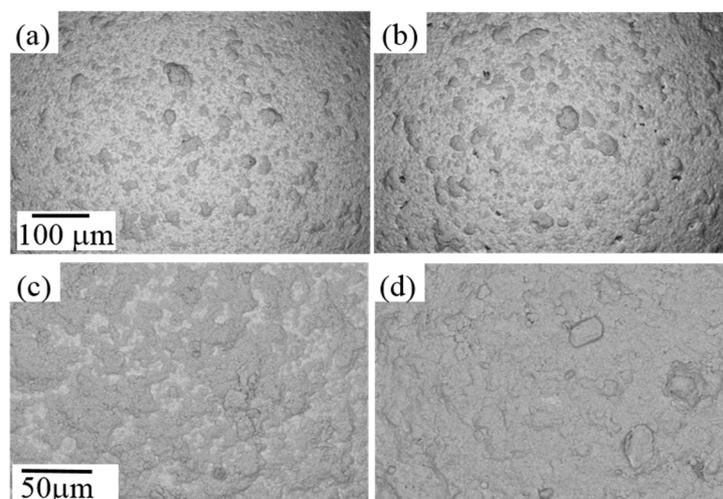


Figure 7. SEM images of morphologies of the samples: (a) TS300-4; (b) TSS300-4; (c) TS300-8; and (d) TSY300-8.

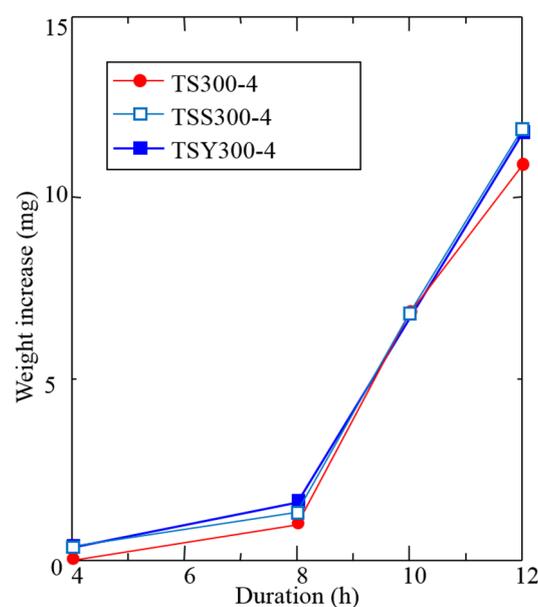


Figure 8. Weight increase of 50 steel balls during mechanical coating versus duration.

3.4. Influence of Substrate Material

We also studied the influence of substrate material on the formation of continuous Ti coatings. When stainless steel (SUS-304) balls were chosen as the substrate (Figure 9), the formation of continuous Ti coatings took about 10 h, which was identical to that using steel (SUJ-2) balls as the substrate. This means that the required time to form continuous Ti coatings on stainless steel and steel balls was identical. However, the formation of continuous Ti coatings on Al_2O_3 balls in the same condition took 20 h [25]. Therefore, we can conclude that the formation of Ti coatings on steel balls is easier and quicker than on ceramic balls. In other words, the substrate plays a key role in the formation of Ti coatings. From the above results, we can state that the formation of Ti coatings on steel balls is much easier and quicker than on ceramic balls. The influence of substrate material on the formation of metallic coatings can be explained as follows.

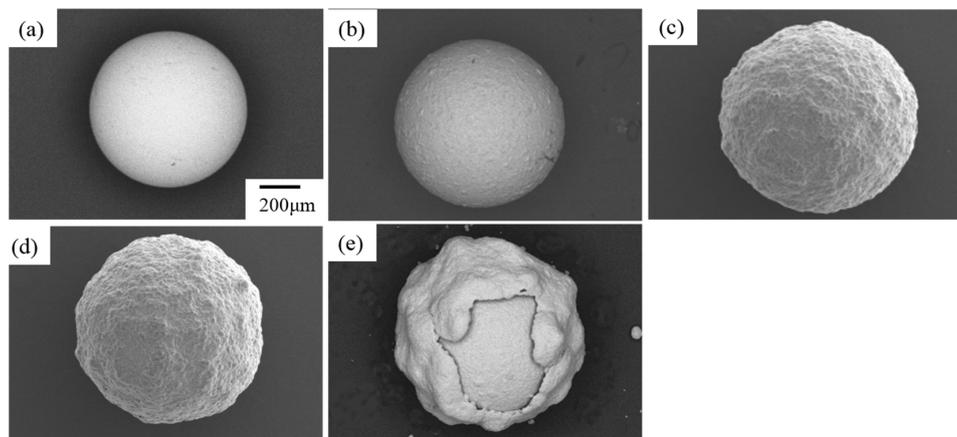


Figure 9. SEM images of surface morphologies of Ti coatings on stainless steel (SUS-304) balls prepared by mechanical coating at 300 rpm after different duration: (a) 0 h; (b) 4 h; (c) 10 h; (d) 16 h and (e) 60 h.

Firstly, it is well-known that the hardness of Al_2O_3 is about 2300 HV, which is far greater than those of steel and stainless steel. When substrate hardness decreased from 2300 HV to 809 HV, the required time to form continuous Ti coatings decreased from 20 h to 10 h. With a further decrease of substrate hardness from 809 HV to 187 HV, the required time hardly decreased, indicating that decreasing the substrates' hardness within a certain range can shorten the formation of Ti coatings. The influence of substrate hardness has been discussed above. Secondly, the material transfer from metal to ceramics is difficult than cold welding between metal materials [26]. Some works [24,26] have proved that the interaction between metallic particles and ceramic balls belongs to mechanical self-locking due to the plastic deformation of metallic particles. However, the cold welding occurred among the fresh surface of the balls and metallic powder particles when balls became metallic ones. The strength of self-locking is lower than that of cold welding.

4. Conclusions

Continuous Ti coatings on steel and stainless steel ball substrates were prepared by mechanical coating technique. Greater revolution speed, providing larger collision force and energy, accelerated the formation of continuous Ti coatings. The substrate material plays an essential role in the formation of Ti coatings; specifically, Ti coatings or even other metal coatings are more easily formed on metal/alloy balls than on ceramic balls. Meanwhile, substrate hardness also markedly affected the formation of Ti coatings. The material with smaller surface hardness is more suitable as the substrate on which Ti coatings were prepared. The above conclusion can also be exerted on other metal or alloy coatings on metal/alloy and ceramic substrates.

Acknowledgments: This work is financially supported by the National Nature Science Foundation of China (No. 51404170), the Innovation Team Program of Tianjin University of Science & Technology (No. 10117) and the Scientific Research Foundation of Tianjin University of Science & Technology (No. 10220).

Author Contributions: Y. Lu conceived and designed the experiments; L. Hao performed the experiments; L. Hao and H. Yoshida analyzed the data; T. Itoi contributed analysis tools; L. Hao wrote the paper.

Conflicts of Interest: The authors declare no conflict of interest.

References

1. Ramanauskas, R.; Quintana, P.; Maldonado, L.; Pomés, R.; Pech-Canul, M.A. Corrosion resistance and microstructure of electrodeposited Zn and Zn alloy coatings. *Surf. Coat. Technol.* **1997**, *92*, 16–21. [[CrossRef](#)]
2. Tang, J.J.; Bai, Y.; Zhang, J.C.; Liu, K.; Liu, X.Y.; Zhang, P.; Wang, Y.; Zhang, L.; Liang, G.Y.; Gao, Y.; et al. Microstructural design and oxidation resistance of CoNiCrAlY alloy coatings in thermal barrier coating system. *J. Alloys. Compd.* **2016**, *688*, 729–741. [[CrossRef](#)]
3. Zhou, C.; Zhang, Q.; Li, Y. Thermal shock behavior of nanostructured and microstructured thermal barrier coatings on a Fe-based alloy. *Surf. Coat. Technol.* **2013**, *217*, 70–75. [[CrossRef](#)]
4. Yamamoto, K.; Ito, H.; Kujime, S. Nano-multilayered CrN/BCN coating for anti-wear and low friction applications. *Surf. Coat. Technol.* **2007**, *201*, 5244–5248. [[CrossRef](#)]
5. Wei, S.; Pei, X.; Shi, B.; Shao, T.; Li, T.; Li, Y.; Xie, Y. Wear resistance and anti-friction of expansion cone with hard coating. *Petrol. Explor. Dev.* **2016**, *43*, 326–331. [[CrossRef](#)]
6. Wang, K.; Wang, C.; Yin, Y.; Chen, K. Modification of Al pigment with graphene for infrared/visual stealth compatible fabric coating. *J. Alloys Compd.* **2017**, *690*, 741–748. [[CrossRef](#)]
7. Yoshida, H.; Lu, Y.; Nakayama, H.; Hirohashi, M. Fabrication of TiO₂ film by mechanical coating technique and its photocatalytic activity. *J. Alloys Compd.* **2009**, *475*, 383–386. [[CrossRef](#)]
8. Khosravani, S.; Dehaghi, S.B.; Askari, M.B.; Khodadadi, M. The effect of various oxidation temperatures on structure of Ag-TiO₂ thin film. *Microelectron. Eng.* **2016**, *163*, 67–77. [[CrossRef](#)]
9. Sun, T.; Wang, M. Low-temperature biomimetic formation of apatite/TiO₂ composite coatings on Ti and NiTi shape memory alloy and their characterization. *Appl. Surf. Sci.* **2008**, *255*, 396–400.
10. Cotelan, N.; Rak, M.; Bele, M.; Cör, A.; Muresan, L.; Milošev, I. Sol-gel synthesis, characterization and properties of TiO₂ and Ag-TiO₂ coatings on titanium substrate. *Surf. Coat. Technol.* **2016**, *307A*, 790–799. [[CrossRef](#)]
11. He, J.; Luo, Q.; Cai, Q.Z.; Li, X.W.; Zhang, D.Q. Microstructure and photocatalytic properties of WO₃/TiO₂ composite films by plasma electrolytic oxidation. *Mater. Chem. Phys.* **2011**, *129*, 242–248. [[CrossRef](#)]
12. Stojadinović, S.; Radić, N.; Vasilčić, R.; Petković, M.; Stefanov, P.; Zeković, L.; Grbić, B. Photocatalytic properties of TiO₂/WO₃ coatings formed by plasma electrolytic oxidation of titanium in 12-tungstosilicic acid. *Appl. Catal B Environ.* **2012**, *126*, 334–341. [[CrossRef](#)]
13. Ghicov, A.; Macak, J.M.; Tsuchiya, H.; Kunze, J.; Haeublein, V.; Frey, L.; Schmuki, P. Ion implantation and annealing for an efficient N-doping of TiO₂ nanotubes. *Nano Lett.* **2006**, *6*, 1080–1082. [[CrossRef](#)]
14. Schlott, F.; Ohser-Wiedemann, R.; Jordan, T.; Kreisel, G. Effect of the electrolyte composition on the anatase fraction of photocatalytic active TiO₂ coatings prepared by plasma assisted anodic oxidation. *Thin Solid Films* **2012**, *520*, 2549–2553. [[CrossRef](#)]
15. Lu, Y.; Matuszaka, K.; Hao, L.; Hiraoka, Y.; Yoshida, H.; Pan, F. Photocatalytic activity of TiO₂/Ti composite coatings fabricated by mechanical coating technique and subsequent heat oxidation. *Mater. Sci. Semicond. Proc.* **2013**, *16*, 1949–1956. [[CrossRef](#)]
16. Guan, S.; Hao, L.; Lu, Y.; Yoshida, H.; Pan, F.; Asanuma, H. Fabrication of oxygen-deficient TiO₂ coatings with nano-fiber morphology for visible-light photocatalysis. *Mater. Sci. Semicond. Proc.* **2016**, *41*, 358–363. [[CrossRef](#)]
17. Lu, Y.; Hirohashi, M.; Zhang, S. Fabrication of oxide film by mechanical coating technique. In Proceedings of the International Conference on Surface, Coatings and Nanostructured Materials, Aveiro, Portugal, 7–9 September 2005. Paper No. FP117.
18. Kobayashi, K. Formation of coating film on milling balls for mechanical alloying. *Mater. Trans.* **1995**, *36*, 134–137. [[CrossRef](#)]

19. Romankov, S.; Sha, W.; Kaloshkin, S.D.; Kaevitser, K. Formation of Ti-Al coatings by mechanical alloying method. *Surf. Coat. Technol.* **2006**, *201*, 3235–3245. [[CrossRef](#)]
20. Gupta, G.; Mondal, K.; Balasubramaniam, R. In situ nanocrystalline Fe-Si coating by mechanical alloy. *J. Alloys Compd.* **2009**, *482*, 118–122. [[CrossRef](#)]
21. Farahbakhsh, I.; Zakeri, A.; Manikandan, P.; Hokamoto, K. Evaluation of nanostructured coating layers formed on Ni balls during mechanical alloying of Cu powder. *Appl. Surf. Sci.* **2011**, *257*, 2830–2837. [[CrossRef](#)]
22. Hao, L.; Lu, Y.; Asanuma, H.; Guo, J. The influence of the processing parameters on the formation of iron thin films on alumina balls by mechanical coating technique. *J. Mater. Process. Technol.* **2012**, *212*, 1169–1176. [[CrossRef](#)]
23. Hao, L.; Lu, Y.; Sato, H.; Asanuma, H. Fabrication of zinc coatings on alumina balls from zinc powder by mechanical coating technique and the process analysis. *Powder Technol.* **2012**, *228*, 377–384. [[CrossRef](#)]
24. Lü, L.; Lai, M.; Zhang, S. Modeling of the mechanical-alloy process. *J. Mater. Process. Technol.* **1995**, *52*, 539–546. [[CrossRef](#)]
25. Lu, Y.; Guan, S.; Hao, L.; Yoshida, H. Review on the photocatalyst coatings of TiO₂: Fabrication by mechanical coating technique and its application. *Coatings* **2015**, *5*, 545–556. [[CrossRef](#)]
26. Hao, L.; Lu, Y.; Sato, H.; Asanuma, H.; Guo, J. Influence of metal properties on the formation and evolution of metal coatings during mechanical coating. *Metall. Mater. Trans. A* **2013**, *44*, 2717–2724. [[CrossRef](#)]



© 2017 by the authors. Licensee MDPI, Basel, Switzerland. This article is an open access article distributed under the terms and conditions of the Creative Commons Attribution (CC BY) license (<http://creativecommons.org/licenses/by/4.0/>).